

G-MATT: Single-step Retrosynthesis Prediction using Molecular Grammar Tree Transformer

Kevin Zhang^{a,*}, Vipul Mann^{b,*}, Venkat Venkatasubramanian^{b,**}

^a*Department of Computer Science, Columbia University, New York, USA*

^b*Department of Chemical Engineering, Columbia University, New York, USA*

Abstract

In recent years, several reaction templates-based and template-free approaches have been reported for single-step retrosynthesis prediction. Even though many of these approaches perform well from traditional data-driven metrics standpoint, there is a disconnect between model architectures used and underlying chemistry principles governing retrosynthesis. Here, we propose a novel chemistry-aware retrosynthesis prediction framework that combines powerful data-driven models with chemistry knowledge. We report a tree-to-sequence transformer architecture based on hierarchical SMILES grammar trees as input containing underlying chemistry information that is otherwise ignored by models based on purely SMILES-based representations. The proposed framework, grammar-based molecular attention tree transformer (G-MATT), achieves significant performance improvements compared to baseline retrosynthesis models. G-MATT achieves a top-1 accuracy of 51% (top-10 accuracy of 79.1%), invalid rate of 1.5%, and bioactive similarity rate of 74.8%. Further analyses based on attention maps demonstrate G-MATT’s ability to preserve chemistry knowledge without having to use extremely complex model architectures.

1. Introduction

Predicting chemical reaction outcomes and retrosynthesis planning are leading challenges in computational chemistry despite the growing interest in this field, ease of availability of more computation power, and significant developments in data-driven modeling, including the recent surge of large language models (LLMs). The implications of accurately modeling chemical reactions are significant with widespread implications in – drug discovery and development, materials design,

* Authors contributed equally

** Corresponding author

Email address: venkat@columbia.edu (Venkat Venkatasubramanian)

catalysis, polymer design, reducing environmental impact of existing materials, and so on. It has been argued that developing hybrid approaches that combine data-driven approaches with chemistry knowledge is required for wider adoption [1, 2].

There are two aspects to the reaction modeling problem – first, forward prediction, involving predicting the reaction product given a set of reactant molecules, and second, retrosynthesis prediction, involving predicting precursors required to synthesize a given target molecule. While both the problems are challenging and require learning complex interactions between molecules to identify the correct target molecule(s), the retrosynthesis prediction problem is relatively more difficult due to its combinatorial nature – at each step, several synthesis pathways are usually possible and the entire sequence of synthesis pathways are required to be predicted correctly. Moreover, in a single-step retrosynthesis problem, multiple synthesis pathways are approximated by a single step synthesis pathway (from target molecule to precursors in one step), making it an even more difficult problem. In this work, our focus is to develop such single-step models for retrosynthesis (or inverse) reaction prediction.

Single-step models could be classified as either template-based or template-free. Template-based models use predefined reaction templates to categorize and predict chemical reaction pathways. These templates are obtained through either data-driven approaches or designed using human expertise. One of the first template-based retrosynthesis models was LHASA [3] which incorporated chemical templates through reaction logic and heuristics. More recently, Synthia (formerly known as Chematica) [4] is another such template-based approach developed using a decision tree approach that selects a reaction template from 70,000 expert created rules. Other template-based approaches for synthesis planning are presented in [5–7]. On the other hand, recent advancements in computational power and machine learning have spurred a focus on template-free models. Template-free models use purely data-driven approaches to plan and evaluate reaction pathways and address some limitations of template-based methods such as lack of generality of prediction and dependence on template-quality. These methods typically represent molecules as strings in simplified molecular-input line-entry system (SMILES) format and model the reaction prediction problem as a sequence-to-sequence (seq2seq) problem. One of the earliest such works is by Liu et al. [8]. Recently, owing to the success of the state-of-the-art transformer architecture [9], a molecular transformer model was proposed [10] for forward prediction with significant performance improve-

ment over other approaches [11–13]. Similarly, for the retrosynthesis problem, transformer-based approaches have been shown to be promising [14–17]. Other applications of SMILES-based representations include property prediction [18–20], molecular design and optimization [21], studying chemical reaction networks [22] and computer-aided chemical product design [23]. The reader is referred to [1] for a detailed presentation and comparison of various template-based, template-free, and hybrid approaches for computer-aided reaction prediction and chemical synthesis.

While the vast majority of sequence-to-sequence models use the SMILES representation to represent input and target molecules, there are several limitations with using purely text-based SMILES representations in sequence modeling frameworks. First, molecules are treated as merely character-based strings, disregarding the additional structural aspects. Second, the SMILES representation does not provide *explicit* structural information on the nature of chemical bonds, chains, atoms, and so on. Third, the underlying rules characterizing a SMILES string are disregarded and it is left upon the model to identify these patterns to ensure syntactically correct SMILES strings during prediction. These issues were addressed in our prior work on forward prediction [24] and retrosynthesis prediction [25] by using text-based representations generated from the underlying SMILES grammar (instead of just SMILES). Using SMILES grammar-based representations are akin to providing more syntactic as well as semantic information about a molecule’s SMILES representation, resulting in chemistry-rich representations that explicitly contain additional structural information. We have shown in our previous works that the SMILES grammar-based text representation leads to improved accuracy, fewer model parameters, and lower conditional entropy from an information-theoretic standpoint [24, 25]. Our proposed SMILES grammar-based molecular representation is a new and promising alternative to the SMILES representation where the molecules are initially represented as hierarchical tree.

In this work, we propose a tree-to-sequence transformer architecture which explicitly incorporates the hierarchical tree structure of the grammar-based representation of molecules. In the previous methods [24, 25], we utilized a vanilla sequence-to-sequence transformer architecture that required the hierarchical tree to be converted to a sequence, thus breaking the natural hierarchical tree structure of the SMILES grammar which might be beneficial for the model performance. On the contrary, the customized tree-transformer model proposed in this work preserves the hierarchy to the fullest extent while feeding the molecule to the model. Inclusion of such hierarchical structure

results in significant performance improvement compared to the baseline models. This architecture also overcomes the syntactic fragility of the grammar-trees, improving the percentage of syntactically valid predictions compared to the baseline models. Thus, the major contributions of our work could be summarized as below:

- Developed a customized tree-transformer model that takes SMILES grammar-based tree representation(s) of molecule(s) as input, taking into account the tree hierarchy to the fullest extent
- Incorporated chemistry-knowledge through tree convolution blocks (TCB) that performs convolution operations on the grammar tree akin to functional groups in group contribution theory
- Reported significant improvement in model accuracy and decrease in incorrect predictions when compared to the baseline models with incorrect predictions having high bioactive similarity with ground truth

The rest of the paper is organized as follows. In Section 2, we formulate retrosynthesis and forward reaction prediction and conceptually motivate the tree-to-sequence transformer model. We present the methods of our work, including the SMILES grammar, tree-to-sequence transformer, and beam search decoding strategy in Section 3. In Section 4, we introduce the datasets and model training and hyperparameter tuning strategy. The evaluation metrics, results, and analysis of our model appear in Section 5. Lastly, we summarize our major contributions in Section 6.

2. Problem formulation and motivation

2.1. Retrosynthesis

We formulate the retrosynthesis prediction problem as a tree-to-sequence modeling problem where the input molecule (or set of molecules) are represented as SMILES grammar-based trees and the target molecule(s) are represented using their SMILES string(s). Thus, this results in a tree-to-sequence modeling problem, as opposed to the commonly used sequence-to-sequence modeling. To the best of our knowledge, this is the first attempt to develop a tree-to-sequence approach for

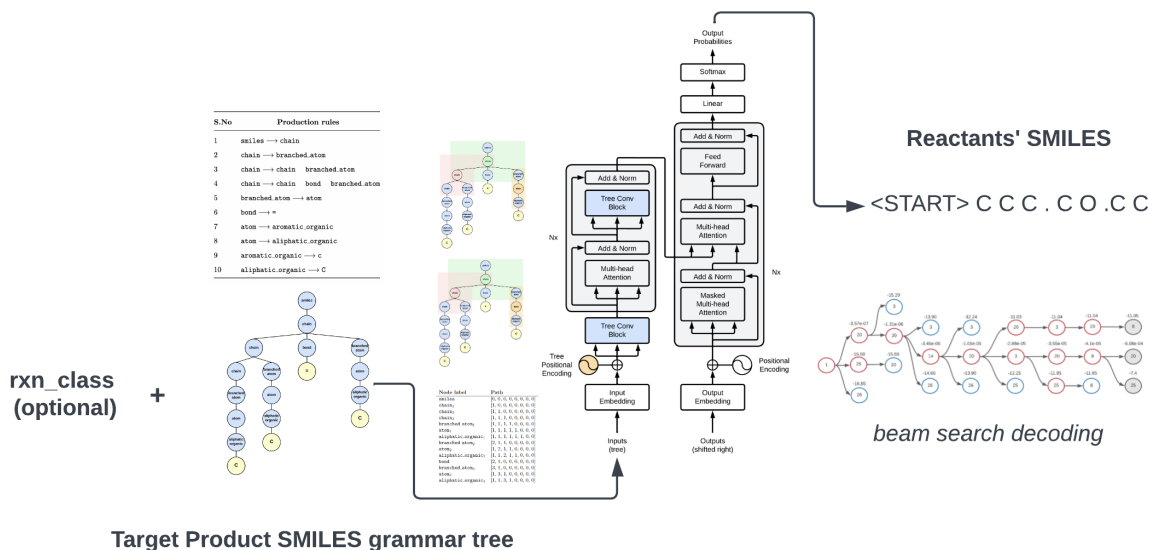


Figure 1: Overview of the proposed tree2smiles approach with SMILES grammar tree of the target molecule as input to predict SMILES strings of the set of precursors.

modeling retrosynthesis and forward reaction prediction problems. The problem formulation is shown in Figure 1 below.

For the retrosynthesis problem, there are two scenarios that need to be modeled – known reaction class and unknown reaction class. For the known reaction class case, a reaction class identifier is appended to the beginning of the target molecule to indicate reaction class type; for the unknown reaction class case, only the target molecule is given as input. Since there may be multiple reactants in the predicted pathway, we use a special character ‘.’ as a delimiter to separate precursors (reactants) on the right hand side and a special <START> token is used to begin the translation process.

2.2. Tree-to-sequence model architecture

Our prior work proposed on grammar-based approach for retrosynthesis [25] and forward prediction [24] used the vanilla sequence-to-sequence transformer for neural machine translation. This requires the SMILES grammar trees to be converted to a sequence of tokens by parsing the tree nodes in a depth-first manner. While the tokens in the grammar-based representation provide more structural information about the molecule, this method discarded any hierarchical structure while flattening the tree. To ensure the transformed model has more explicit and direct access to the grammar tree structure, we add two components to the vanilla transformer commonly used in tree-

based code analysis and generation – tree positional encodings and tree convolutional blocks. A high level comparison of the seq2seq and tree2seq transformers is shown schematically in Figure 2.

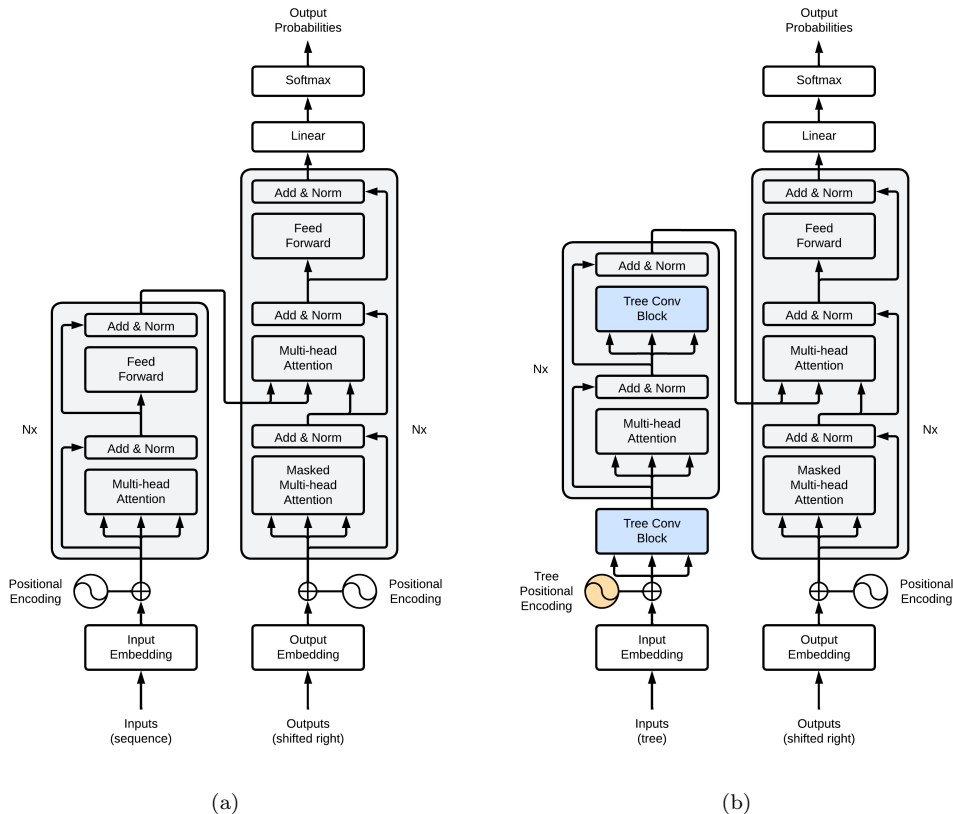


Figure 2: A schematic comparison of the vanilla sequence-to-sequence transformer in (a) and our tree-to-sequence transformer in (b). The two new components in the tree2seq transformer are the tree positional encoding (orange) and tree convolution block (blue). The tree positional encoding replaces the sequential encoding in the encoder and the TCB replaces the feed forward network in the encoder only.

Tree positional encodings, introduced in [26], replace sequential positional encodings in the vanilla transformer in the encoder. While sequential position encodings are suitable for sequential input, it is suboptimal for hierarchical input since each encoding should indicate the positional of a node in the tree rather than its position in the flattened sequence. Similarly, tree convolutional blocks (or TCBs) proposed in [27] provides nodes with information about their parent and children nodes, giving each node progressively more information on the nodes and sub-trees around it. An attention mechanism computes the attention scores between local structures in the grammar tree. These local structures in the tree are akin to functional groups in group contribution theory, so the attention sublayer has more direct access to the underlying chemistry. Further details on tree positional encodings and tree convolutional blocks are presented in Section 3.3 and Section 3.4,

respectively.

3. Methods

In this section, we present the background methods of our tree-to-sequence based approach for retrosynthesis. This includes the SMILES grammar-based molecular tree representations, modifications to the original transformer architecture (including tree positional encodings and convolutional blocks), and the beam search decoding procedure used for predicting the most likely target sequences for a given input sequence.

3.1. SMILES grammar

We treat SMILES strings-based representation of molecules [28] as a formal language where each character is analogous to a word and each string is analogous to a sentence. This enables the use of context-free grammar (CFG) to represent the molecule. The idea behind context-free grammars is that sentences can be built recursively from smaller phrases and these constituents can be grouped according to a semantic hierarchy. Formally, a context-free grammar (V, Σ, R, S) consists of a start symbol S , a set of terminal symbols Σ , a set of non-terminal symbols V , and a set of product rules R . Each production rule is of the form $A \rightarrow \alpha$, where $A \in V$ is a non-terminal symbol and α is a string of terminals or non-terminal symbols.

A context-free grammar for the SMILES representation of molecules comprises characters in the SMILES strings as terminal symbols and meta-information about molecular structure as non-terminal symbols. We provide a representative subset of the SMILES grammar used in our work in Table 1. The symbols defining the CFG in this example are

- S : smiles
- Σ : { =, c, C }
- V : { chain, branched_atom, bond, atom, aromatic_organic, aliphatic_organic }
- R : production rules 1 through 10 in Table 1

Table 1: Simplified SMILES grammar.

S.No	Production rules
1	<code>smiles</code> \rightarrow <code>chain</code>
2	<code>chain</code> \rightarrow <code>branched_atom</code>
3	<code>chain</code> \rightarrow <code>chain</code> <code>branched_atom</code>
4	<code>chain</code> \rightarrow <code>chain</code> <code>bond</code> <code>branched_atom</code>
5	<code>branched_atom</code> \rightarrow <code>atom</code>
6	<code>bond</code> \rightarrow <code>=</code>
7	<code>atom</code> \rightarrow <code>aromatic_organic</code>
8	<code>atom</code> \rightarrow <code>aliphatic_organic</code>
9	<code>aromatic_organic</code> \rightarrow <code>c</code>
10	<code>aliphatic_organic</code> \rightarrow <code>C</code>

We leverage the underlying SMILES grammar to provide information about the structure and composition of a molecule in its grammar-based representation. Consider propene, with the SMILES string representation given by `CC=C`. This representation could be obtained by applying the set of production rules in Table 1 to obtain the corresponding parse-tree shown in Figure 3.

Compared to a purely character-based SMILES string, the SMILES grammar tree-based representations incorporate more chemical and structural information which is then leveraged by the model architecture for better performance. In our previous works, we have shown that these representations are more efficient in modeling the underlying chemistry, eliminate overparameterization in complex machine learning architectures [24], and are superior from an information-theoretic standpoint [25].

3.2. Tree-to-sequence transformer

We model the reaction prediction as a sequence modelling problem using a tree-to-sequence transformer that predicts a sequence-based output from a tree-based input. For this task, we use a modified state-of-the-art sequence-to-sequence transformer that can handle tree hierarchical input data as shown in Figure 2 above. The vanilla and tree-to-sequence transformer frameworks both consist of an encoder-decoder architecture where the encoder maps the input sequence to a latent space from which a decoder autoregressively decodes the latent representation to predict the output

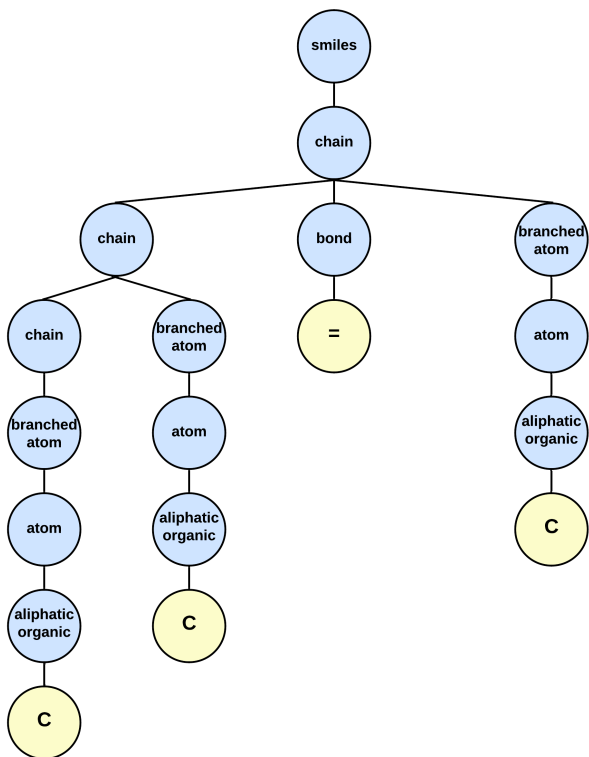


Figure 3: The grammar tree for propene CC=C with the SMILES tokens as leaf nodes and the hierarchical structure containing the production rules and non-terminal symbols characterizing the molecular structural aspects. We use such hierarchical SMILES grammar trees as input combined with tree positional encodings and convolutional blocks to extract contextual information.

sequence. The modifications from the original transformer architecture are the tree positional encodings and convolutional block sublayers, described in detail in the following sections.

In the tree-to-sequence transformer, we preserve the attention-mechanism, which lets the transformer determine relationships between tokens in an input sequence. We use the ‘Scaled-Dot Product Attention’ introduced in [9], which uses a set of queries, keys, and values vectors. The query and key vectors are of dimensions d_k and the value vector is of dimension d_v . The attention score then is computed as softmax function applied over the dot-products of the queries and key vectors, scaled down by a factor of $\sqrt{d_k}$, given by

$$\text{Attention}(Q, K, V) = \text{softmax} \left(\frac{QK^T}{\sqrt{d_k}} \right) V,$$

where Q , K , and V are the matrices of query, key, and values vectors, respectively. The attention score computed above determines the importance of different parts of an input sequence in

the current context. In order to allow the model to jointly factor in information from different representation subspaces at different positions, multi-headed attention is computed, which involves computing multiple attention scores in parallel, which are then concatenated and projected using a linear transformation to compute the multi-head attention scores as,

$$\text{MultiHead}(Q, K, V) = (\text{head}_1 \parallel \text{head}_2 \parallel \dots \parallel \text{head}_h)W^O,$$

where $\text{head}_i = \text{Attention}(QW_i^Q, KW_i^K, VW_i^V)$, and $W_i^Q \in \mathbb{R}^{d_{pos} \times d_k}$, $W_i^K \in \mathbb{R}^{d_{pos} \times d_k}$, $W_i^V \in \mathbb{R}^{d_{pos} \times d_v}$ are the projection matrices for Q , K , and V respectively.

3.3. Tree Positional Encodings

The original transformer paper [9] creates sequential positional encodings using sinusoidal functions of varying frequencies. These positional encodings are added to the embeddings in the encoder and decoder to provide the model information about input order. However, flattening the grammar tree into a sequence does not preserve hierarchical information about the tree. Parents and children may be separated by long distances in the sequential representation. Conversely, consecutive tokens in the flattened tree sequence may be far apart in the grammar tree. To address these problems and better preserve hierarchical tree structure, we use tree positional encodings introduced in [26] which are based on the sinusoidal encodings in the original transformer.

For retrosynthesis, let the input grammar tree $T = (V, E, r)$ consist of a set of nodes V , edges E , and a root node r . For all $v \in V$, the path from r to v can be uniquely identified by an edge path $p_v \in \mathbb{Z}_{\geq 0}^L$ of length L according to the following definition:

- $p_r = 0_L$, where 0_L is the vector of length L of all zeros.
- Otherwise, v has a parent node p with N children v_1, v_2, \dots, v_N . Suppose $v_k = v$. Then, $p_v = k \parallel \pi_{L-1}(p_p)$, where \parallel denotes vector concatenation and $\pi_{L-1}(p_p)$ denotes the first $L - 1$ elements of p_p .

We depict the edge paths for each node in the example grammar tree in Figure 4b. For each node, the edges corresponding to each child is labeled with their child index (k in the above definition). Note that the root node `smiles` is a vector of all zeros and that every child node shares its parent node path shifted to the right by one.

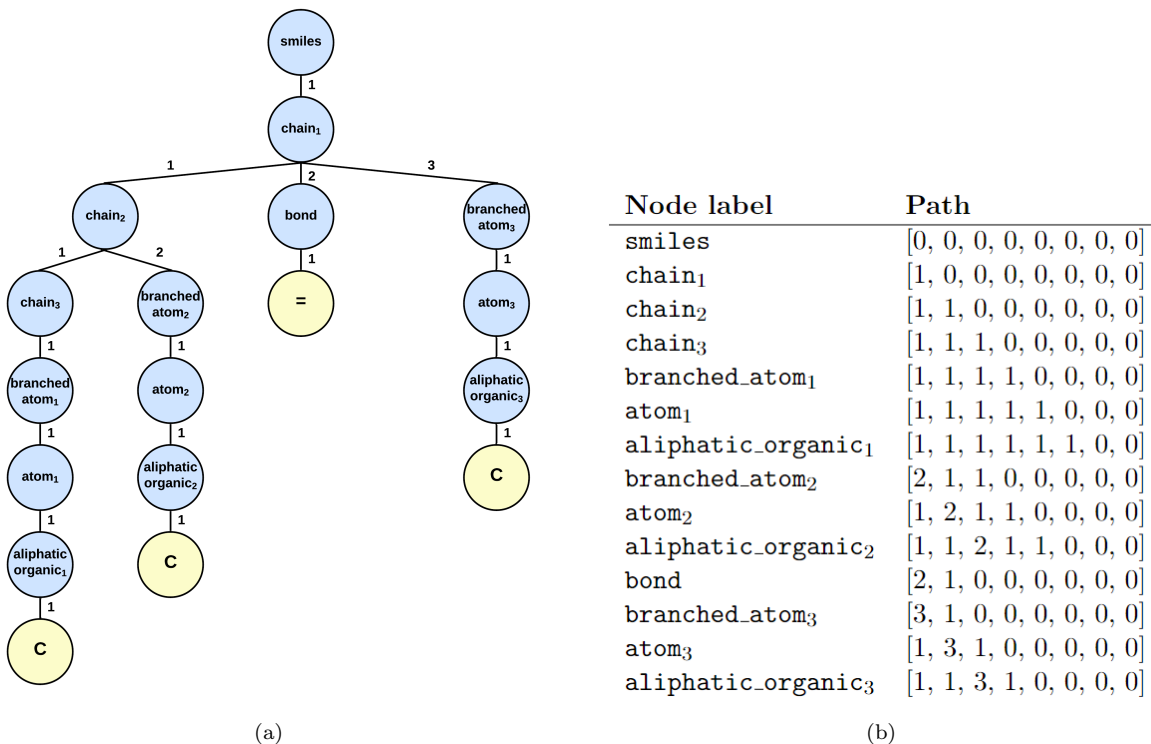


Figure 4: The tree paths for the example grammar tree for propene CC=C. The grammar tree with edge labels is shown in (a) and the corresponding edge paths with $L = 8$ for each node in (b). The subscripts in the node labels are solely to distinguish between different nodes with same labels.

To encode the position of the node v , we apply the sinusoidal positional encodings in [9] to each element in the edge path p_v to obtain an edge embedding. For all $v \in V, \ell \in \{1, \dots, L\}$,

$$EE_{v,\ell,2i} = \sin(\omega_i \cdot (p_v)_\ell)$$

$$EE_{v,\ell,2i+1} = \cos(\omega_i \cdot (p_v)_\ell)$$

with $w_i = 1/10000^{2i/d}$ for $i \in \{1, \dots, \frac{d}{2}\}$. The parameter d is the dimension of the edge embedding i.e. $EE_{v,\ell,2i} \in \mathbb{R}^d$. The tree positional encoding of v is the concatenation of the edge embeddings in the edge path p_v .

$$TE_v = EE_{v,1} \parallel \dots \parallel EE_{v,L}.$$

This results in an positional encoding of dimension $d \cdot L$, which also corresponds to the model size d_m , or the dimension of the node embedding in the model.

The proposed tree positional encodings have several desirable properties as shown in [26]. Like the original sequential encodings, tree encodings satisfy uniqueness. This is because the edge path

from the root r to a node v is unique and the sinusoidal encodings are injective for each frequency ω_i due to the transcendental property of π . Furthermore, the encoding of a child node will share the first $d \cdot (L - 1)$ dimensions with encoding of the parent node, shifted right by d dimensions. Combined with the uniqueness property, this shifting property enables to model to determine if a node is an ancestor or sibling of another node. Finally, due to the mathematical properties of sine and cosine, given the encoding for an edge $(p_v)_\ell$, the encoding for a sibling edge $(p_v)_\ell + k$ can be computed by a linear combination of trigonometric functions.

3.4. Tree Convolutional Block

Inspired by [27], we introduce a modified Tree Convolutional Block (TCB) architecture to the tree2seq transformer to handle tree-structured data. The block allows each node access to information about its parents and children, thereby explicitly incorporating tree-structured information to the model. The TCB replaces the encoder feed forward sublayer after the attention sublayer in the original transformer in [9]. In addition to using a TCB at each sublayer, we add a TCB following the positional encoding in the encoder. This layer combines the embeddings from the parent, children, and current node before any self-attention. The decoder does not include the TCB since it decodes a sequence of SMILES tokens and thus does not require tree information.

Given a node x , let x_t and x_p be the representation of the current and parent node respectively. Furthermore, let x_c be the average of the representation of all the children nodes. Formally, if x has children $x_{c_1}, x_{c_2}, \dots, x_{c_N}$, then $x_c = \frac{1}{N} \sum_{i=1}^N x_{c_i}$. The single-layer tree convolution block for x is then computed as

$$TCB_1(x_t, x_p, x_c) = \text{relu}(x_t W_t + x_p W_p + x_c W_c) W_2 + b_2.$$

If the current node does not have a parent or children nodes, then x_p and x_c are replaced with a special learned vector v_p and v_c respectively. The TCB may be generalized to multiple layers, where an L -layer TCB consists of L consecutively stacked single-layer tree convolutions blocks. For our model, we use $L = 2$ for all TCBs.

The single-layer TCB incorporates information of all nodes that are distance at most one from the current node. Hence, the L -layer TCB includes information about all nodes of distance at most L away. Thus, increasing the depth of the TCB increases the width of local tree structure made

explicitly available to the model.

We modify the original TCB architecture in [27] by using the children nodes rather than the left-sibling in the convolution since this change performed better experimentally. We propose two reasons to explain this behavior. First, by using children nodes, information flows up and down the tree rather than only upwards. Second, production rules in the grammar have few children, typically at most two, so sibling order information has relatively low importance. This also suggests that averaging children node representation sufficiently preserves information about the children. In Figure 5, we show the behavior of the TCB on the example grammar tree for propene. Each colored region shows the convolution window around the node of the same corresponding color. Note that with the TCB, the model has explicit information about the local structures around each node. This prior chemistry knowledge enables the architecture to more easily model relationships between molecules as it has more structural information.

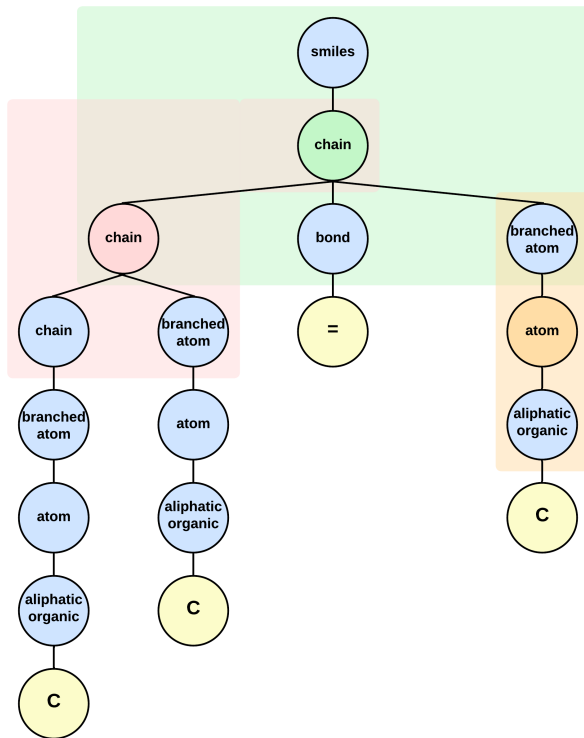


Figure 5: The grammar tree for propene CC=C and three example convolution windows in red, green, and orange. Each convolution window operates on the respectively colored node, thereby providing the node with information about its parent and children.

3.5. Beam search

In order to evaluate the transformer performance during inference, we use a beam search decoding strategy to autoregressively predict the output. Beginning with a <START> token, the transformer decodes the next token from the latent space with the current predicted sequence as input. The beam search procedure of size B determines the set of top- B tokens at each step based on their likelihood and saves the top- B sequences as the next search frontier. If $B = 1$, then the transformer employs a greedy strategy which involves selecting the maximum likelihood token at each decoding step. Using beam search allows us to evaluate our model’s performance more extensively and compare it with the top-K accuracy reported in other similar works in this area. A schematic of the beam-search decoding procedure is shown in Figure 6.

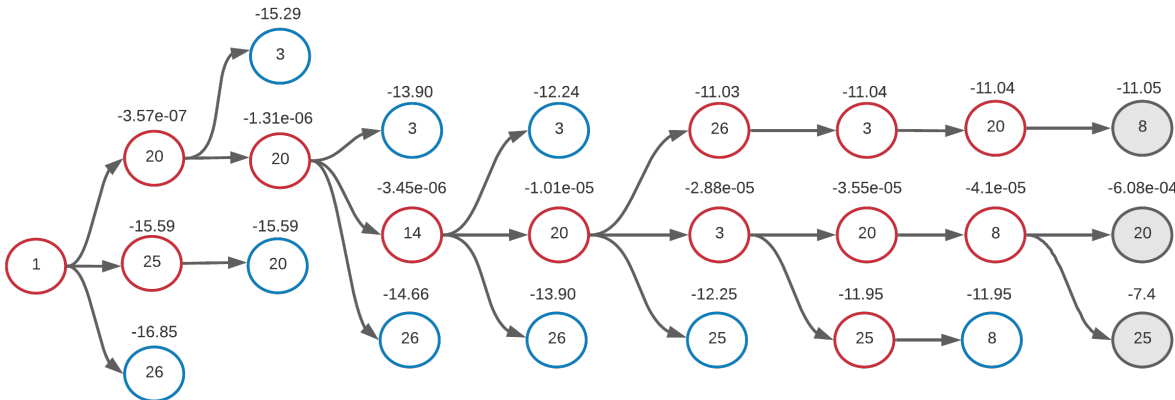


Figure 6: A schematic for a partially completed beam search procedure with beam size $B = 3$. At each decoding step, the 3 most likely sequences are preserved and used as the search frontier. The B most likely tokens for each sequence is computed and the top- B sequences are used for the next step. The completed sequences are then used to reconstruct the corresponding SMILES string. The log-likelihood values are indicated above each node in the schematic.

4. Dataset and model training

In this section, we provide details on the datasets used for training the retrosynthesis models along with details on the model training aspects.

4.1. Dataset

We work with the USPTO-50K retrosynthesis prediction dataset, a filtered subset of the US Patents and Trademark Office’s (USPTO) database [29] and further classified into ten different reaction classes [30]. The filtered dataset contains only the reactants and products, with the reagent

information removed and the SMILES strings canonicalized. This is a standard dataset used for benchmarking the performance of retrosynthesis models reported in literature and allows for training of both known and unknown reaction class scenarios. Since our approach is based on generating SMILES grammar-based tree representations, we parse the input molecules’ SMILES strings in the database using the SMILES grammar described in Section 3.1. This implies that certain molecules may not be *in grammar* and are not included in the model training stage. Note that expanding the grammar’s scope to include these molecules is trivial and could be done by adding rules corresponding to additional elements such as Si, Pt, Zn, Mg, and so on. Table 2 summarizes the reaction database with the number of reactions that are in grammar along with the train, validation, and test-set splits.

Table 2: An overview of the retrosynthesis dataset

Dataset	train	valid	test	total
USPTO-50K (retrosynthesis)				
with (sanitized) molecules				50,037
in grammar	38,899	4,849	4,846	48,594

4.2. Model training

We train the transformer models using a cross-entropy-based loss function. The models were trained using the Adam optimizer [31] with beta $\beta_1 = 0.9$, $\beta_2 = 0.98$, and $\epsilon = 10^{-9}$, and a triangular cyclic learning rate schedule proposed in [32] that is characterized by a max learning rate $\eta_{max} = 5 \times 10^{-4}$, min learning rate $\eta_{min} = 1 \times 10^{-4}$. For retrosynthesis, we use $n = 10$ epochs per cycle and learning rate decay per cycle $\gamma = 0.98$. At the training stage, to avoid overfitting, a dropout layer is used for both the attention-mechanism and TCB with probability $p = 0.2$. A loss function based on sparse categorical cross-entropy between the predicted and actual target sequences is minimized. The lengths of the input and output representations to the model are fixed at 350 and 121, respectively. The representation lengths were fixed based on the longest representation lengths in the training set.

The retrosynthesis model for known reaction class was trained for 250 epochs and for the unknown reaction class for 190 epochs. All models were trained using TensorFlow 2.1 and python

3.7. For generating the parse-trees and extracting grammar-based features, we used the Natural Language ToolKit (NLTK) 3.4.5 library. The molecular datasets were processed using the 2019 release of the RDKit library.

5. Results

In this section, we present the test-set performance of the trained models. We first define the model evaluation metrics for retrosynthesis prediction, benchmark the performance compared to other similar works in this area, and highlight the advantages and current limitations of our framework.

Since a product may have multiple correct retrosynthesis pathways, we not only measure if the predicted reaction is an exact match to the ground truth, but also if the precursor molecules are chemically similar. Chemically similar molecules are likely to produce feasible and correct reactions in practice. Hence, we include metrics based on chemical similarity as it provides a more comprehensive and practical evaluation of the model.

To determine chemical similarity, we use the Tanimoto index, which is one of the most commonly used and best metrics to compute structural similarity between molecules [33]. The Tanimoto coefficient T_c is a value between 0 and 1 which indicates the fraction of common molecular fingerprints between two molecules. Given two molecules X and Y with fingerprint sets A and B , the Tanimoto coefficient is computed as

$$T_c(X, Y) = \frac{A \cap B}{A + B - A \cup B}.$$

Two molecules will have a coefficient of zero if they have no common fingerprints and two identical molecules will have a coefficient of one. Although there is no coefficient which distinguishes similar and non-similar molecules, we use the common threshold $T_c = 0.85$ for bioactive similarity. In other words, we consider two molecules bioactively similar if their Tanimoto score satisfies $0.85 \leq T_c \leq 1$.

5.1. Evaluation metrics

We define the following performance metrics: accuracy, fractional accuracy, MaxFrag accuracy, MaxFrag bioactive similarity rate (BASR), and invalid rate. Accuracy measures the fraction of reactions in which the precursor molecules are perfectly predicted; fractional accuracy measures the fraction of ground truth precursor molecules predicted correctly; MaxFrag accuracy is the prediction

accuracy of the maximal fragment (longest precursor molecule based on SMILES length); MaxFrag BASR is the fraction of reactions in which the predicted maximal fragment is bioactively similar ($0.85 \leq T_c \leq 1$) to the ground truth maximal fragment; and invalid rate measures the percentage of syntactically/grammatically invalid SMILES predictions. A schematic demonstrating these metrics for an example molecule in the test-set is shown in Figure 7 below.

Based on Figure 7, we observe that even though a prediction could be chemically correct, it is still considered incorrect if it doesn't exactly match the set of precursors in the ground truth set. For instance, the most likely prediction (prediction 1) matches the ground truth precursors and hence is correct. However, the second most likely prediction (prediction 2) contains a fluorine (F) instead of bromine (Br) for one of the precursors and even though these are chemically correct (both are halogens), they are still considered incorrect while computing accuracy. Thus, the reported exact-match accuracy is a lower bound on the model performance and in practice, the actual performance is likely to be better than expected based only on exact-match accuracy.

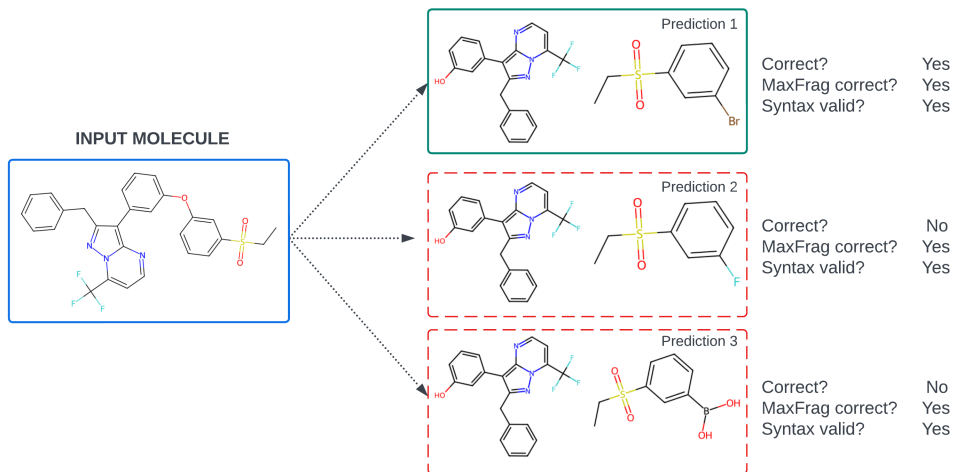


Figure 7: Top-3 predictions generated by our model for a given input molecule in the test-set. The first (most-likely) prediction matches the ground truth, the second is chemically feasible but incorrect since it doesn't exactly match the ground truth, and third prediction seems chemically incorrect. All predictions are syntactically valid and has correctly predicted maximal fragment.

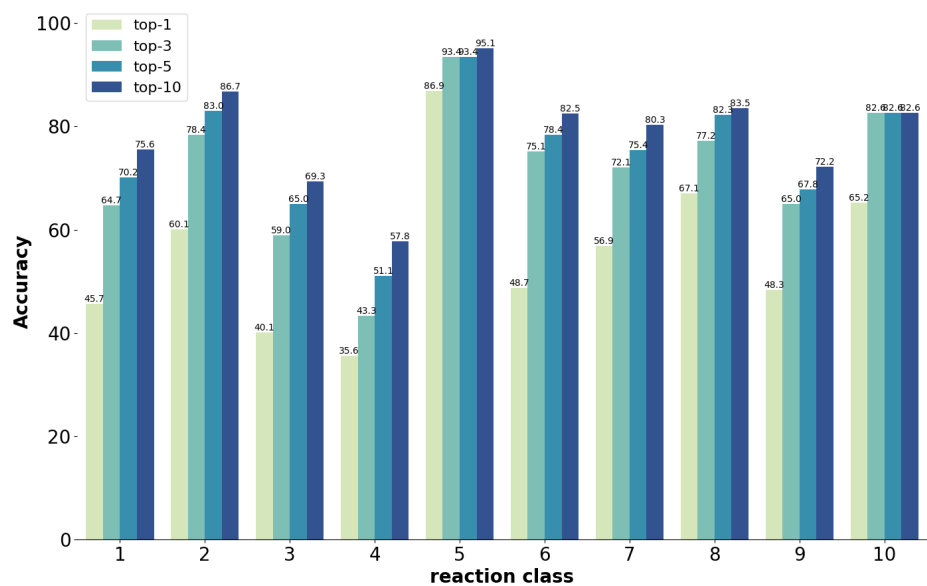
5.2. Retrosynthesis prediction

Performance evaluation metrics. The performance evaluation measures computed on the test set of the USPTO 50K dataset are presented in Table 3 both for the known and unknown reaction class scenarios.

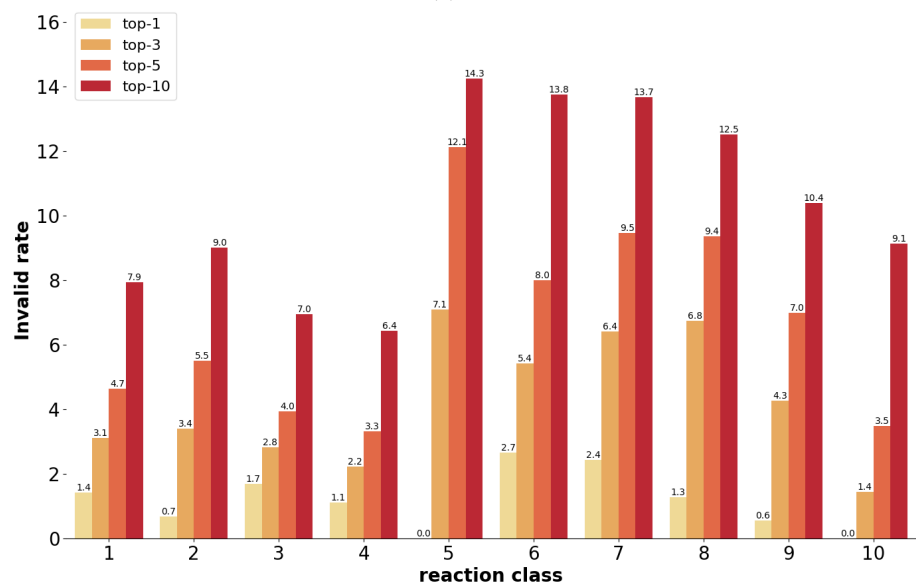
Table 3: Retroynthesis models’ performance metrics on the test set

Performance measure	top-k measure (%)				
	1	2	3	5	10
Known reaction class					
Accuracy	51.0	64.3	70.0	74.6	79.1
Fractional accuracy	64.7	74.9	79.4	83.2	86.8
MaxFrag accuracy	60.6	71.6	76.5	80.4	84.1
MaxFrag BASR	74.8	82.2	85.4	88.3	92.3
Invalid rate	1.5	2.7	4.0	6.0	9.8
Unknown reaction class					
Accuracy	41.6	54.0	60.4	67.6	73.1
Fractional accuracy	52.0	63.7	69.8	76.3	81.3
MaxFrag accuracy	49.0	60.5	66.5	72.7	77.8
MaxFrag BASR	60.0	70.8	76.4	82.2	86.8
Invalid rate	1.3	2.0	2.6	3.8	6.

In addition to evaluating the model on the entire test set, we compute class-wise prediction accuracy and invalid rate for both known and unknown reaction class scenarios in Figure 8 and Figure 9, respectively. The dataset contains reaction across 10 different classes and details on the number of reactions in each class are presented in Appendix 2.

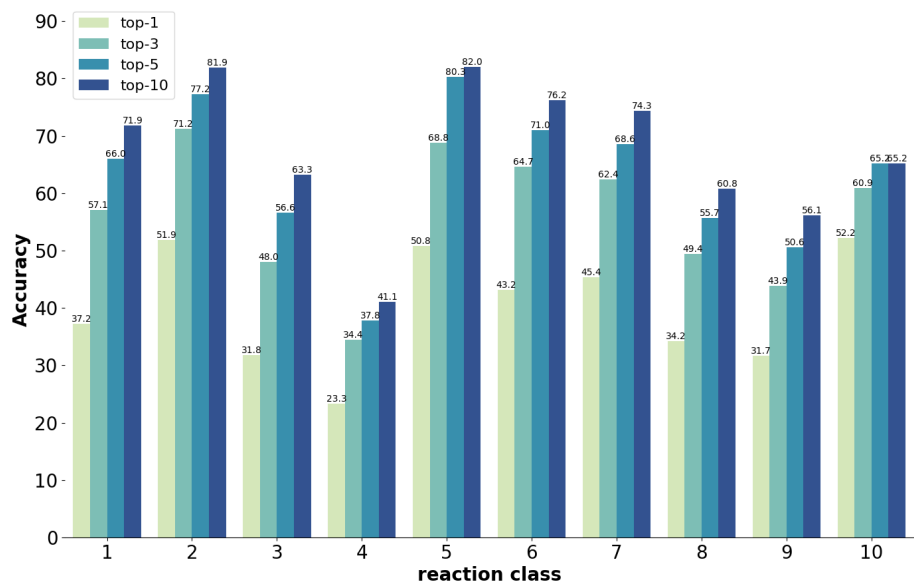


(a)

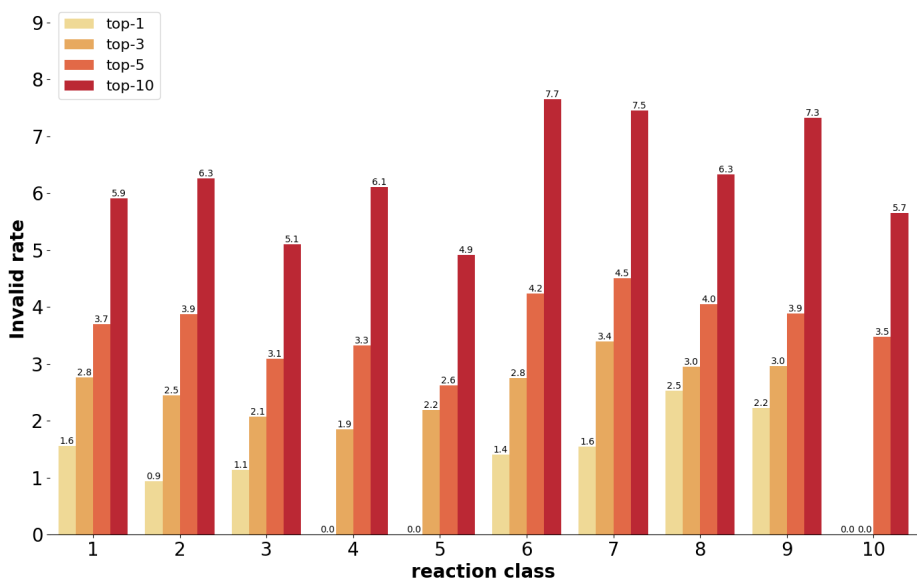


(b)

Figure 8: The class-wise top-1, top-3, top-5, and top-10 prediction accuracy (a) and invalid SMILES string rate (b) for retrosynthesis prediction with known reaction class.



(a)



(b)

Figure 9: The class-wise top-1, top-3, top-5, and top-10 prediction accuracy (a) and invalid SMILES string rate (b) for retrosynthesis prediction with unknown reaction class.

Comparison with other works. Here, we benchmark the performance of our model against other transformer-based approaches reported in literature. We compare the top-k prediction accuracy and the top-k invalid rate to perform a more holistic comparison as shown in Table 4. We observe that both for the known and unknown reaction class cases, the proposed model, G-MATT, attains nearly state-of-the-art performance both on prediction accuracy and invalid rate.

For instance, for the known reaction class scenario, G-MATT’s top-k prediction accuracy is on average within 4.3% of Lin et al.’s state-of-the-art model [34] and outperforms it by 1.25% on average for the invalid rate. Similarly, for the unknown reaction class, G-MATT’s top-k prediction accuracy is on average within 3.1% of Lin et al.’s model and outperforms it by 1.13% on invalid rate. Similarly, compared to SCROP, which comprises an additional transformer model for correcting incorrect predictions made by a primary retrosynthesis transformer model, G-MATT with its single transformer architecture outperforms the prediction accuracy for unknown reaction class case for several top-k values.

We emphasize here that the G-MATT model is relatively simpler compared to other approaches in the literature such as SCROP, tied two-way transformer models, transfer-learning based approaches, and so on, and still, G-MATT attains nearly state-of-the-art performance both on the prediction accuracy as well as the invalid prediction rate. This could be attributed to its following important characteristics – first, richer input representations based on SMILES grammar tree instead of purely linear SMILES strings; second, presence of tree positional encodings to correctly capture the tree hierarchy; and third, tree convolution blocks instead of simple feed-forward networks in the transformer architecture for performing tree convolutions similar to functional groups’ contribution in group contribution theory. Thus, when combined with additional model training strategies reported in prior works in the literature, we envision further improvements in G-MATT model’s performance. Our goal here is not to pursue the state-of-the-art but rather demonstrate the value in using alternative SMILES grammar-based tree representations for the reaction prediction tasks.

Table 4: Comparison with other transformer-based retrosynthesis models trained on USPTO-50K dataset

model	top-k accuracy (%)				top-k invalid rate (%)			
	1	3	5	10	1	3	5	10
Known reaction class								
Liu et al. [35]	37.4	52.4	57.0	61.7	12.2	15.3	18.4	22.0
Grammar seq2seq [25]	43.8	57.2	61.4	66.6	4.4	7.2	8.4	9.6
SCROP [36]	59.0	74.8	78.1	81.1				
Lin et al. [34]	54.3	74.1	79.2	84.4	2.3	4.9	7.0	12.1
T2T [37]	54.1	68.0	69.0	70.1				
G-MATT (proposed)	51.0	70.0	74.6	79.1	1.5	4.0	6.0	9.8
Unknown reaction class								
Liu et al. [35]	28.3	42.8	47.3	52.8				
Grammar seq2seq [25]	32.1	44.3	48.9	54.0	5.1	7.4	8.4	9.7
Chen et al. [38]	39.1	62.5	69.1	74.5				
Karpov et al. [14]	40.6	42.7	63.9	69.8				
SCROP [36]	43.7	60.0	65.2	68.7	0.7	1.4	1.8	2.3
Lin et al. [34]	42.0	64.0	71.3	77.6	2.2	3.7	4.8	7.8
Tied two-way TF [17]	47.1	67.1	73.1	76.3	0.1	0.2	0.6	10.2
G-MATT (proposed)	41.6	60.4	67.6	73.1	1.3	2.6	3.8	6.3

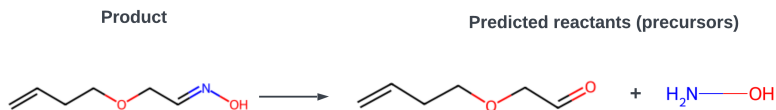
Near-miss predictions. To further analyze the incorrect predictions, we take a closer look at the incorrectly predicted molecules from a chemistry standpoint. We compute the Tanimoto similarity of the incorrectly predicted maximal fragment molecule. Since for the retrosynthesis model there are multiple molecules in the ground truth, without loss of generality, we compute Tanimoto similarity with only the maximal fragment molecule and report aggregated Tanimoto similarity scores for the test-set *incorrect predictions* compared to the ground truth. This exercise would provide us with an indication of the degree of similarity between the incorrectly predicted precursors when compared to the ground truth. Table 5 below shows the percentile splits of incorrect predictions segregated by their Tanimoto similarities.

Model	Tanimoto similarity (%) (incorrect predictions)		
	$0.5 \leq T_c$	$0.7 \leq T_c$	$0.85 \leq T_c$
Known reaction class	66.6	46.8	31.5
Unknown reaction class	78.8	63.7	48.7

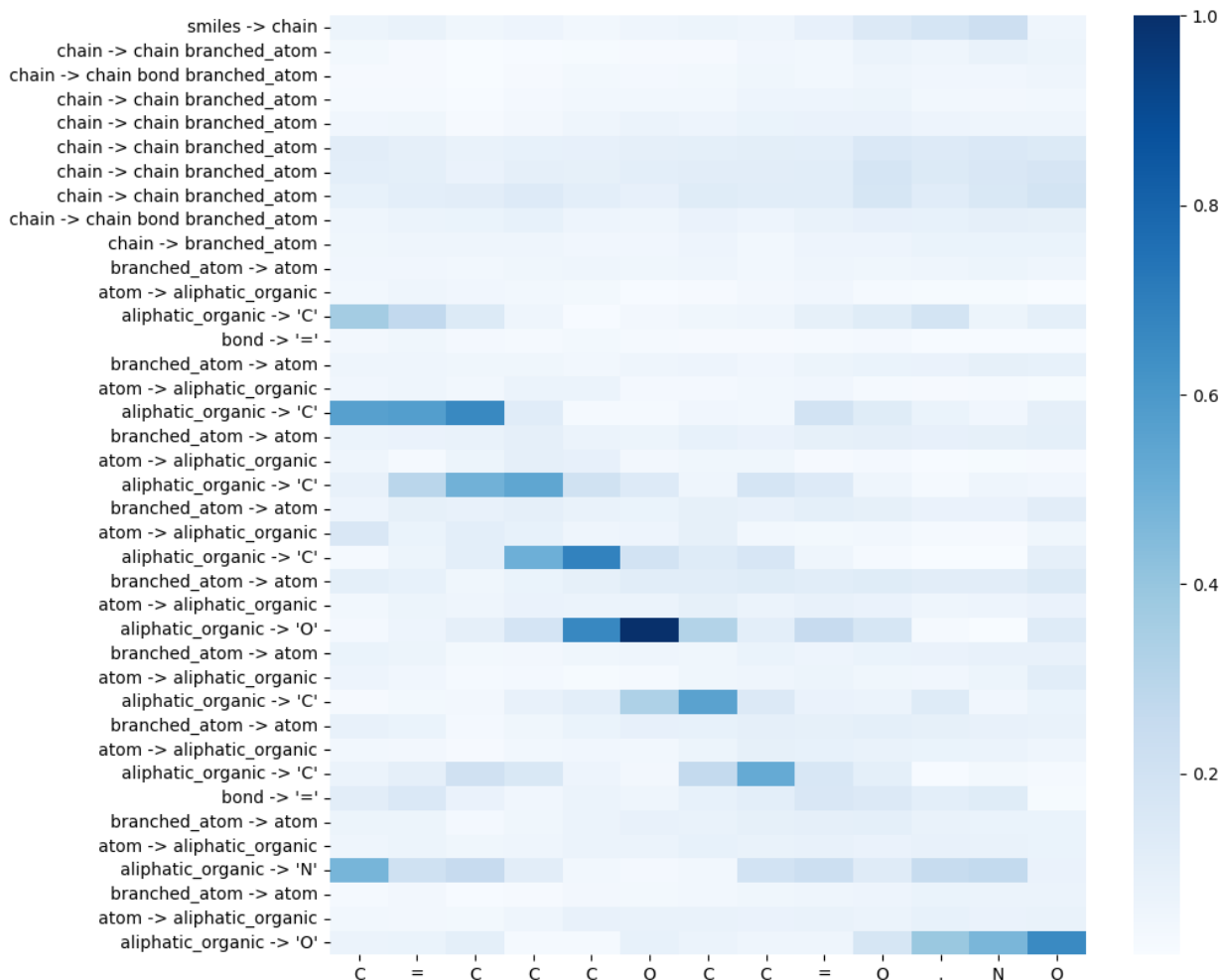
Table 5: Distribution of Tanimoto coefficient scores across *incorrect* top-1 predictions for both the models

Attention-map for molecules. To provide insights on the grammar-based representation of molecules, we analyze the attention weights calculated by the attention sublayers in the transformer. Specifically, we calculate and show the average of the attention scores across all cross-attention modules in the decoder in Figure 10. A higher attention score indicates that two tokens are more strongly related while translating from products to reactants.

As indicated by high attention scores along the diagonal, the attention mechanism is able to identify and map the atoms/bonds in the input molecule to the atoms/bonds in the precursor molecules as they get transformed from products to reactants. Moreover, for the example reaction shown in Figure 10a, the bond disconnection site is the ‘N’ atom in the ‘-N=O’ functional group in the input molecule. From the attention map, we observe that ‘aliphatic_organic → O’ and ‘aliphatic_organic → N’ both have the highest attention scores for ‘.’ token separating precursors – indicating that the model has correctly identified bond disconnection site. This is further confirmed by the additional examples provided in Appendix 3 where the bond disconnection sites (‘aliphatic_organic → S’ in Figure 11 and ‘aromatic_organic → c’ in Figure 12) have the highest attention scores for the ‘.’ token separating precursors. In addition, we also observe that in general, a given atom in the precursor molecule (horizontal axis) has multiple adjacent atoms/bonds corresponding to the product molecule (vertical axis). Similarly, a given atom in the product molecule (vertical axis) has high attention scores for multiple atoms in the precursors molecules (horizontal axis). Both of these observations indicate that owing to the convolutional operations on the hierarchical tree representation, the G-MATT model takes into account the context of neighboring atoms while making predictions and gives importance to the local structures. Furthermore, a general observation is that G-MATT’s attention maps are generally sparse with several input tokens with relatively lower cross-attention scores, pointing towards the efficiency of the tree representation that imposes inherent structure on the tokens. As a result of this, the semantics and syntactical structure of tokens are captured and the model focuses on only the most important tokens to resolve uncertainty while making predictions and the other tokens are inferred from the structural constraints learned. Additional cross-attention maps for the G-MATT model are presented in Appendix 3.



(a) An example top-1 prediction to study the transformer attention map



(b) Average attention scores for top-1 prediction on the retrosynthesis reaction C=CCCOCC=NO -> C=CCCOCC=O.NO extracted from the transformer decoder cross-attention sublayer

Figure 10: Molecular attention map for the SMILES grammar tree of the product and SMILES strings of the reactants (precursors) for an example reaction

6. Conclusions

In this work, we have proposed a novel tree-based transformer architecture for retrosynthesis, allowing for molecular inputs to be represented as hierarchical trees as opposed to linear, text-based SMILES representations. The tree transformer is characterized by tree convolutional operations that allows it to incorporate neighboring context of atoms as functional groups, tree positional encodings

that allow for an explicit representation of tree hierarchy, and SMILES grammar tree of molecules as inputs that allow for utilization of inherent structural information explicitly. We demonstrate that incorporating tree structure in the transformer model explicitly makes use of the advantages of a grammar-based tree representation. We report the top-1 prediction accuracy of 51.0% (top-10 accuracy of 79.1%) and syntactic invalid rate of 1.5%. In the case of incorrect predictions for unknown reaction class, we observe that 48.7% of *incorrectly predicted* MaxFrag precursors were bioactively similar to the ground truth. Moreover, the visualized attention scores illustrated that the model identified reaction centers correctly, takes into account the surrounding context of atoms/bonds while making predictions, and has an efficient attention map due to learned structural constraints. We emphasize here that the G-MATT framework is relatively simple and attains nearly state-of-the-art performance both on prediction accuracy and invalid rate. Thus, when combined with additional model training strategies such as model weights averaging, customized learning schedules, exhaustive hyperparameter search, and so on, we envision further improvements in G-MATT model performance and is part of our future work in this direction.

CRedit authorship contribution statement

Kevin Zhang: Conceptualization, Formal analysis, Writing – original draft, Writing – review & editing. **Vipul Mann:** Conceptualization, Formal analysis, Writing – original draft, Writing – review & editing. **Venkat Venkatasubramanian:** Conceptualization, Writing – review & editing, Supervision, Funding acquisition

Acknowledgements

This work was supported by the U.S. National Science Foundation (NSF) under Grant No. 2132142 and carried out at Columbia University.

Appendix 1: SMILES grammar

The SMILES grammar used in this work is the same as that used in our previous works [24, 25]. This grammar comprises 80 production rules with 24 non-terminals symbols specifying the different structural components of a SMILES string. All the production rules for the grammar used in our work are summarized in Table 6. The first and the last production rules, `SMILES` \rightarrow `CHAIN` and `NOTHING` \rightarrow `NONE`, are additional rules included signifying the start and end of a SMILES string, which is analogous to the `<START>` and `<END>` tokens in natural language processing marking the beginning and the end of sentences, respectively.

Table 6: SMILES grammar used for retrosynthesis and forward reaction prediction. ‘|’ separates multiple production rules applicable for the same non-terminal symbol.

S.No	Production rules
1	<code>SMILES</code> \rightarrow <code>CHAIN</code>
2	<code>ATOM</code> \rightarrow <code>BRACKET_ATOM</code> <code>ALIPHATIC_ORGANIC</code> <code>AROMATIC_ORGANIC</code>
3	<code>ALIPHATIC_ORGANIC</code> \rightarrow <code>B</code> <code>C</code> <code>N</code> <code>O</code> <code>S</code> <code>P</code> <code>F</code> <code>I</code> <code>Cl</code> <code>Br</code>
4	<code>AROMATIC_ORGANIC</code> \rightarrow <code>c</code> <code>n</code> <code>o</code> <code>s</code> <code>p</code>
5	<code>BRACKET_ATOM</code> \rightarrow <code>LEFT_BRACKET</code> <code>BAI</code> <code>RIGHT_BRACKET</code>
6	<code>BAI</code> \rightarrow <code>SYMBOL</code> <code>BAC</code>
7	<code>BAC</code> \rightarrow <code>CHIRAL</code> <code>BAH</code> <code>BAH</code> <code>CHIRAL</code>
8	<code>BAH</code> \rightarrow <code>HCOUNT</code> <code>BACH</code> <code>BACH</code> <code>HCOUNT</code>
9	<code>BACH</code> \rightarrow <code>CHARGE</code>
10	<code>SYMBOL</code> \rightarrow <code>ALIPHATIC_ORGANIC</code> <code>AROMATIC_ORGANIC</code>
11	<code>DIGIT</code> \rightarrow <code>1</code> <code>2</code> <code>3</code> <code>4</code> <code>5</code> <code>6</code> <code>7</code>
12	<code>CHIRAL</code> \rightarrow <code>@</code> <code>@@</code>
13	<code>HCOUNT</code> \rightarrow <code>H</code> <code>H</code> <code>DIGIT</code>
14	<code>CHARGE</code> \rightarrow <code>-</code> <code>+</code>
15	<code>BOND</code> \rightarrow <code>-</code> <code>=</code> <code>#</code> <code>/</code> <code>\</code>
16	<code>RINGBOND</code> \rightarrow <code>DIGIT</code> <code>BOND</code> <code>DIGIT</code>
17	<code>BRANCHED_ATOM</code> \rightarrow <code>ATOM</code> <code>ATOM</code> <code>RB</code> <code>ATOM</code> <code>BB</code> <code>ATOM</code> <code>RB</code> <code>BB</code>
18	<code>RB</code> \rightarrow <code>RB</code> <code>RINGBOND</code> <code>RINGBOND</code>
19	<code>BB</code> \rightarrow <code>BB</code> <code>BRANCH</code> <code>BRANCH</code>
20	<code>BRANCH</code> \rightarrow <code>LEFT_BRACKET</code> <code>CHAIN</code> <code>RIGHT_BRACKET</code> <code>LEFT_BRACKET</code> <code>BOND</code> <code>CHAIN</code> <code>RIGHT_BRACKET</code>
21	<code>CHAIN</code> \rightarrow <code>BRANCHED_ATOM</code> <code>CHAIN</code> <code>BRANCHED_ATOM</code> <code>CHAIN</code> <code>BOND</code> <code>BRANCHED_ATOM</code>

Table 6: SMILES grammar used for retrosynthesis and forward reaction prediction. ‘|’ separates multiple production rules applicable for the same non-terminal symbol.

S.No	Production rules
22	LEFT_BRACKET \rightarrow BRANCHED_ATOM CHAIN BRANCHED_ATOM CHAIN BOND BRANCHED_ATOM
23	RIGHT_BRACKET \rightarrow BRANCHED_ATOM CHAIN BRANCHED_ATOM CHAIN BOND BRANCHED_ATOM
24	NOTHING \rightarrow NONE

Appendix 2: USPTO-50K class-wise distribution

Table 7 summarizes the distribution of the various reactions across the 10 reaction classes for the USPTO-50K dataset (retrosynthesis).

Table 7: Distribution of reactions across different reaction classes that are in-grammar

Rxn class	Rxn name	train	valid	test	total
1	Heteroatom alkylation and arylation	11,886	1,476	1,478	14,840
2	Acylation and related processes	9,358	1,165	1,169	11,698
3	C – C bond formation	4,324	544	539	5,407
4	Heterocycle formation	710	89	90	889
5	Protections	513	64	62	639
6	Deprotections	6,357	796	789	7,942
7	Reductions	3,607	448	452	4,507
8	Oxidations	629	80	79	788
9	Functional group interconversion (FGI)	1,434	176	180	1,790
10	Functional group addition (FGA)	177	23	23	223

References

1. Venkatasubramanian, V. & Mann, V. Artificial intelligence in reaction prediction and chemical synthesis. *Current Opinion in Chemical Engineering* **36**, 100749 (2022).
2. Mann, V., Gani, R. & Venkatasubramanian, V. Group contribution-based property modeling for chemical product design: A perspective in the AI era. *Fluid Phase Equilibria*, 113734 (2023).
3. Pensak, D. A. & Corey, E. J. in (ACS Publications).
4. Szymkuć, S., Gajewska, E. P., Klucznik, T., Molga, K., Dittwald, P., Startek, M., Bajczyk, M. & Grzybowski, B. A. Computer-Assisted Synthetic Planning: The End of the Beginning. *Angewandte Chemie International Edition* **55**, 5904–5937 (2016).
5. Coley, C. W., Rogers, L., Green, W. H. & Jensen, K. F. Computer-assisted retrosynthesis based on molecular similarity. *ACS central science* **3**, 1237–1245 (2017).
6. Law, J., Zsoldos, Z., Simon, A., Reid, D., Liu, Y., Khew, S. Y., Johnson, A. P., Major, S., Wade, R. A. & Ando, H. Y. Route designer: a retrosynthetic analysis tool utilizing automated retrosynthetic rule generation. *Journal of chemical information and modeling* **49**, 593–602 (2009).
7. Nicolaou, C. A., Watson, I. A., LeMasters, M., Masquelin, T. & Wang, J. Context aware data-driven retrosynthetic analysis. *Journal of Chemical Information and Modeling* **60**, 2728–2738 (2020).
8. Liu, B., Ramsundar, B., Kawthekar, P., Shi, J., Gomes, J., Luu Nguyen, Q., Ho, S., Sloane, J., Wender, P. & Pande, V. Retrosynthetic Reaction Prediction Using Neural Sequence-to-Sequence Models. *ACS Central Science* **3**. PMID: 29104927, 1103–1113 (2017).
9. Vaswani, A., Shazeer, N., Parmar, N., Uszkoreit, J., Jones, L., Gomez, A. N., Kaiser, L. & Polosukhin, I. in *Advances in Neural Information Processing Systems 30* (eds Guyon, I., Luxburg, U. V., Bengio, S., Wallach, H., Fergus, R., Vishwanathan, S. & Garnett, R.) 5998–6008 (Curran Associates, Inc., 2017).
10. Schwaller, P., Laino, T., Gaudin, T., Bolgar, P., Hunter, C. A., Bekas, C. & Lee, A. A. Molecular transformer: a model for uncertainty-calibrated chemical reaction prediction. *ACS central science* **5**, 1572–1583 (2019).

11. Nam, J. & Kim, J. Linking the neural machine translation and the prediction of organic chemistry reactions. *arXiv preprint arXiv:1612.09529* (2016).
12. Jin, W., Coley, C. W., Barzilay, R. & Jaakkola, T. *Predicting Organic Reaction Outcomes with Weisfeiler-Lehman Network* 2017.
13. Coley, C. W., Jin, W., Rogers, L., Jamison, T. F., Jaakkola, T. S., Green, W. H., Barzilay, R. & Jensen, K. F. A graph-convolutional neural network model for the prediction of chemical reactivity. *Chemical science* **10**, 370–377 (2019).
14. Karpov, P., Godin, G. & Tetko, I. V. *A transformer model for retrosynthesis in International Conference on Artificial Neural Networks* (2019), 817–830.
15. Tetko, I. V., Karpov, P., Van Deursen, R. & Godin, G. State-of-the-art augmented NLP transformer models for direct and single-step retrosynthesis. *Nature communications* **11**, 1–11 (2020).
16. Wang, X., Li, Y., Qiu, J., Chen, G., Liu, H., Liao, B., Hsieh, C.-Y. & Yao, X. RetroPrime: A Diverse, plausible and Transformer-based method for Single-Step retrosynthesis predictions. *Chemical Engineering Journal* **420**, 129845 (2021).
17. Kim, E., Lee, D., Kwon, Y., Park, M. S. & Choi, Y.-S. Valid, Plausible, and Diverse Retrosynthesis Using Tied Two-Way Transformers with Latent Variables. *Journal of Chemical Information and Modeling* **61**, 123–133 (2021).
18. Mann, V., Brito, K., Gani, R. & Venkatasubramanian, V. Hybrid, interpretable machine learning for thermodynamic property estimation using grammar2vec for molecular representation. *Fluid Phase Equilibria* **561**, 113531 (2022).
19. Goh, G. B., Hodas, N. O., Siegel, C. & Vishnu, A. Smiles2vec: An interpretable general-purpose deep neural network for predicting chemical properties. *arXiv preprint arXiv:1712.02034* (2017).
20. Zhou, Z., Eden, M. & Shen, W. Treat Molecular Linear Notations as Sentences: Accurate Quantitative Structure–Property Relationship Modeling via a Natural Language Processing Approach. *Industrial & Engineering Chemistry Research* **62**, 5336–5346 (2023).

21. Pogány, P., Arad, N., Genway, S. & Pickett, S. D. De novo molecule design by translating from reduced graphs to SMILES. *Journal of chemical information and modeling* **59**, 1136–1146 (2018).
22. Mann, V. & Venkatasubramanian, V. AI-driven hypergraph network of organic chemistry: network statistics and applications in reaction classification. *Reaction Chemistry & Engineering* (2023).
23. Liu, Q., Zhang, L., Liu, L., Du, J., Tula, A. K., Eden, M. & Gani, R. OptCAMD: an optimization-based framework and tool for molecular and mixture product design. *Computers & Chemical Engineering* **124**, 285–301 (2019).
24. Mann, V. & Venkatasubramanian, V. Predicting chemical reaction outcomes: A grammar ontology-based transformer framework. *AIChE Journal* **67**, e17190 (2021).
25. Mann, V. & Venkatasubramanian, V. Retrosynthesis prediction using grammar-based neural machine translation: An information-theoretic approach. *Computers & Chemical Engineering* **155**, 107533 (2021).
26. Thellmann, K.-D., Stadler, B., Usbeck, R. & Lehmann, J. Transformer with Tree-order Encoding for Neural Program Generation (2022).
27. Harer, J., Reale, C. & Chin, P. Tree-Transformer: A Transformer-Based Method for Correction of Tree-Structured Data (2019).
28. Weininger, D. SMILES, a chemical language and information system. 1. Introduction to methodology and encoding rules. *Journal of Chemical Information and Computer Sciences* **28**, 31–36 (1988).
29. Lowe, D. M. *Extraction of chemical structures and reactions from the literature* PhD thesis (University of Cambridge, 2012).
30. Schneider, N., Stiefl, N. & Landrum, G. A. What’s what: The (nearly) definitive guide to reaction role assignment. *Journal of chemical information and modeling* **56**, 2336–2346 (2016).
31. Kingma, D. P. & Ba, J. *Adam: A Method for Stochastic Optimization* 2014.
32. Howard, J. & Ruder, S. Universal language model fine-tuning for text classification. *arXiv preprint arXiv:1801.06146* (2018).

33. Bajusz, D., Rácz, A. & Héberger, K. Why is Tanimoto index an appropriate choice for fingerprint-based similarity calculations? *Journal of cheminformatics* **7**, 1–13 (2015).
34. Lin, K., Xu, Y., Pei, J. & Lai, L. Automatic retrosynthetic route planning using template-free models. *Chemical Science* **11**, 3355–3364 (2020).
35. Liu, B., Ramsundar, B., Kawthekar, P., Shi, J., Gomes, J., Luu Nguyen, Q., Ho, S., Sloane, J., Wender, P. & Pande, V. Retrosynthetic reaction prediction using neural sequence-to-sequence models. *ACS central science* **3**, 1103–1113 (2017).
36. Zheng, S., Rao, J., Zhang, Z., Xu, J. & Yang, Y. Predicting Retrosynthetic Reactions Using Self-Corrected Transformer Neural Networks. *Journal of Chemical Information and Modeling* **60**. PMID: 31825611, 47–55 (2020).
37. Duan, H., Wang, L., Zhang, C., Guo, L. & Li, J. Retrosynthesis with attention-based NMT model and chemical analysis of “wrong” predictions. *RSC Advances* **10**, 1371–1378 (2020).
38. Chen, B., Shen, T., Jaakkola, T. S. & Barzilay, R. Learning to make generalizable and diverse predictions for retrosynthesis. *arXiv preprint arXiv:1910.09688* (2019).